

UNCLASSIFIED

Defense Technical Information Center
Compilation Part Notice

ADP023768

TITLE: Large Eddy Simulations of Bluff-Body Stabilized Turbulent Flames and Gas Turbine Combustors

DISTRIBUTION: Approved for public release, distribution unlimited

This paper is part of the following report:

TITLE: Proceedings of the HPCMP Users Group Conference 2007. High Performance Computing Modernization Program: A Bridge to Future Defense held 18-21 June 2007 in Pittsburgh, Pennsylvania

To order the complete compilation report, use: ADA488707

The component part is provided here to allow users access to individually authored sections of proceedings, annals, symposia, etc. However, the component should be considered within the context of the overall compilation report and not as a stand-alone technical report.

The following component part numbers comprise the compilation report:

ADP023728 thru ADP023803

UNCLASSIFIED

Large Eddy Simulations of Bluff-Body Stabilized Turbulent Flames and Gas Turbine Combustors

S. James, J. Zhu, and M.S. Anand
Rolls-Royce Corporation, Indianapolis, IN
{sunil.james, jiang.zhu, m.s.anand}@rolls-royce.com

B. Sekar
US Air Force Research Laboratory, Propulsion
Directorate, Turbine Engine Division
(AFRL/PRTC), Wright-Patterson AFB, OH
balu.sekar@wpafb.af.mil

Abstract

The paper presents applications of the large eddy simulation (LES) methodology on the Sandia/Sydney turbulent bluffbody burner and gas turbine combustors. LES of the bluffbody flame is performed using the filtered density function (FDF) submodel and a comprehensive augmented chemical mechanism for the first time. The FDF submodel is a sophisticated turbulent-combustion submodel that directly computes the joint probability density function (PDF) of scalars and is therefore considered to be more accurate than conventional assumed-PDF type models. The chemical kinetics mechanism involves 19 species and 15 reaction-steps. The mechanism contains both C1 and C2 species and also involves NO formation steps. Owing to the complexity of the mechanism, numerical integration of the kinetics equations is performed using the in situ adaptive tabulation (ISAT) scheme. Mean velocity and species/temperature fields are presented and compared to experimental data. Results show that the computations are in good agreement with data. The paper also presents LES of a gas turbine combustor. LES is performed using an assumed FDF turbulent-combustion model in conjunction with the flamelet-generated manifold method. The advantage of this approach is that the chemical reaction is parameterized by only two variables, mixture fraction and progress variable. Thus calculations are significantly faster than those with the transport FDF model. Circumferentially averaged combustor exit fuel-air ratio profiles are compared to measurement data for two liner port patterns. It is shown that the LES calculations are in reasonable agreement with data and superior to Reynolds averaged Navier-Stokes calculations. These calculations indicate that LES of practical combustion systems are feasible economically and can be used for design analyses more routinely.

1. Introduction

Traditionally, computational modeling of turbulent reacting flows has been mainly performed using Reynolds-Averaged Navier-Stokes (RANS) methods. However, deficiencies of RANS methods for swirling recirculating flows including gas turbine combustor flows are becoming increasingly apparent. LES offers significant advantages, in that, it captures turbulent mixing and unsteady flow features accurately. In LES, a filtering operation^[1] is performed on the governing equations such that only large-scale flow features are resolved on the computational mesh, while the small-scale features are modeled. The advantage of this approach is that, if one could afford a fine-enough mesh, then theoretically, very little modeling would be required in the calculation. The disadvantage of this method is that a typical LES computational mesh is significantly larger than a typical RANS mesh, and computationally expensive, relatively. However, advances in computational modeling and the availability of cheap distributed computing platforms have made it affordable to use LES for complex geometries^[2-5]. In recent years, LES has become a serious candidate for analyzing reacting flows where the main focus of interest is in regions away from solid boundaries.

Although LES produces better predictions of isothermal flows as compared to RANS, modeling is still needed in LES for accurate predictions of combusting flows. Combustion occurs at the very small scales that are not resolved on the computational mesh. Hence, in addition to the subgrid turbulence models, subgrid combustion models are also required to account for the influence of unresolved scales of the flow on the mean (or filtered) reaction rates. There are several combustion models proposed for LES. Assumed FDF methods^[6] are the most widely used because of their fast turnaround time. In these methods, the reaction is parameterized by one or two variables such as mixture fraction and/or

progress variable. The shape of the FDF of these variables is assumed a priori. With the information available on the FDF, the mean reaction rates can be easily computed. However, applications of assumed-FDF methods are limited to reacting flows that are far from extinction/ignition. This limitation can, in principle, be overcome by transport FDF methods^[7-9]. These methods are considered to be the most sophisticated and can be applied to a variety of reacting flows, such as premixed, partially premixed and nonpremixed combustion systems. In transport FDF methods, the joint FDF of reacting scalars is directly computed via a FDF transport equation. The advantage of these methods is that the closure term related to reaction rates is obviated. Also, chemical kinetics equations of arbitrary complexity can be easily used. Due to the complexity of performing LES/FDF calculations, applications of this methodology to practical flames have been limited. Nevertheless, there is a need to fully understand the predictive capabilities of this model.

This paper presents an evaluation of the FDF model on a standard benchmark bluffbody stabilized flame (Sandia/Sydney Hydrogen/Methane flame [HM1]^[10]) with a comprehensive augmented reduced mechanism. This mechanism allows the computations of major and minor species and overall provides a more realistic representation of the chemical processes in comparison to simple global mechanisms. However, due to the large number of species and reaction steps involved, integration of complex mechanisms is computationally expensive. The *in situ* adaptive tabulation (ISAT) scheme^[11] helps to alleviate this problem and allows the use of such mechanisms at an affordable cost. The paper presents the velocities, species and temperature fields from calculations and compares them with experimental data.

The second part of the paper presents LES of a gas turbine combustor. The subgrid combustion model used in these calculations is based on an assumed FDF method. LES is linked to a spray transport and evaporation model and simulations of two combustor configurations are presented. Circumferentially averaged fuel-air ratio profiles at the combustor exit are compared with rig measurements.

The paper is organized as follows. Section 2 of the paper discusses the numerical methodology and combustion models. Section 3 presents results for the bluffbody flame. Section 4 presents LES of the gas turbine combustors and Section 5 presents the overall findings of this study.

2. Numerical Methodology and Combustion Models

The LES flow solver is based on a pressure-based, low Mach number, collocated, finite-volume solver^[2], to

compute velocity fields. The numerical scheme is an energy-conserving scheme that is second order accurate in space and time. Convective and diffusive terms in the momentum equations are discretized using a central scheme and time derivative is discretized using a second-order backward difference scheme. The subgrid scale stress model used is based on the dynamic model. Convective terms in the scalar transport equations are discretized using the hybrid linear-parabolic approximation scheme in order to prevent unphysical overshoots and undershoots of the scalar fields. The flow solver is linked to combustion models described below.

A. FDF Transport Model

The FDF transport equation is given as References 7-9:

$$\frac{\partial}{\partial t}(F_L) + \frac{\partial}{\partial x_i} \langle u_i \rangle_L F_L = \frac{\partial}{\partial \psi_\alpha} \left(\left\langle \frac{1}{\rho} \frac{\partial}{\partial x_i} J_i^\alpha \right\rangle_L \psi \right) F_L - \frac{\partial}{\partial x_i} \left[\langle u_i \psi \rangle_L - \langle u_i \rangle_L \psi \right] F_L - \frac{\partial}{\partial \psi_\alpha} (S_\alpha F_L) \quad (1)$$

where,

$$F_L(\psi, x; t) = \int_{-\infty}^{+\infty} \rho(x', t) \delta[\psi - \phi(x, t)] G(x' - x) dx' \quad (2)$$

In Eqs. (1) and (2), F_L is the filtered density function, $\langle \rangle_L$ is the conditional expectation, $\langle \rangle_L$ is the Favre filtered mean, ρ is the density, δ is the Dirac-delta function, u_i is the instantaneous velocity, J_i^α is the diffusional flux of species α , S_α is the chemical source term for species α , ψ is the chemical composition in scalar space, ϕ is the chemical composition in physical space, and G is the filter kernel. In Eq. (1), the molecular mixing term (first term on the right side) is typically modeled using the interaction by exchange with mean mixing model. The turbulent convection term (second term on the right side) is modeled by the gradient diffusion model. In Eq. (1), it can be seen that the last term on the right side is due to chemical reactions and is in closed form. Thus reactions of arbitrary complexity can be implemented to describe the chemical processes. Given this advantage of the FDF method and also the fact that the FDF is not specified a priori as in assumed-FDF models, it is expected that the LES/FDF method will yield better predictions of not only overall turbulent flame structures, but also local extinction and reignition scenarios in these flames.

The large dimensionality of Eq. (1) precludes the use of finite-difference or finite-volume schemes for the solution of this equation. Monte-Carlo methods are typically used to solve such equations. In Monte-Carlo

methods, the FDF in each computational cell is represented by an ensemble of notional particles, each with a set of scalars and position vector. The transport of these particles in physical and compositional space mimics the solution of Eq. (1). The mean velocities needed for the transport of these particles are computed by an Eulerian flow solver. Favre filtered scalar values in a cell are computed by ensemble averaging the particle scalar values in the cell.

B. Assumed-FDF Model with the Flamelet-Generated Manifold Method

In contrast to transported FDF methods, in assumed FDF methods^[6], the shape of the FDF is assumed a priori. In the present assumed FDF method, two scalar variables are considered—fuel mixture fraction and a progress variable. This allows the use of this method for partially premixed flames commonly observed in gas turbine combustion systems. The progress variable is typically considered to be a linear combination of species. In the present study, the progress variable is considered to be CO₂. Within the flow-solver, transport equations for mixture-fraction, mixture-fraction variance, progress-variable and progress-variable variance are solved. The mixture fraction FDF is represented by a beta function parameterized by mean and variance. The progress-variable FDF is represented by a tri-delta function, also parameterized by mean and variance. The chemical source terms in the progress-variable and variance of progress-variable transport equations are computed via the flamelet-generated manifold methodology^[12]. In this methodology, it is assumed that a low-dimensional reaction manifold exists in the composition space, and that a reaction path would move towards the manifold and subsequently remain on this manifold. The manifold is generated by performing unstrained premixed flame calculations for different mixture-fraction values using detailed chemical kinetics. The chemical structure of the flame is parameterized by mixture fraction and progress variable. The advantage of this approach is that the source terms can be pre-tabulated (before the LES is performed) in terms of mean and variance of mixture-fraction and progress-variable. During the LES calculation, linear interpolation can be used to compute the source terms. The assumed FDF method is therefore computationally cheap and well suited for routine practical applications.

3. Sandia/Sydney Bluff-Body Stabilized Flame (HM1)

The HM1 burner^[10] consists of a central jet of methane/hydrogen (1:1 volume ratio) surrounded by a bluffbody. The bluffbody is immersed in a coflowing air stream. The diameter of the central jet and the bluffbody are 3.6 mm and 50 mm, respectively. The bulk velocities of the two streams are 118 m/s and 40 m/s, respectively.

LES of the burner is performed on a $136 \times 102 \times 102$ computational mesh (1.4 million grid points) that starts at the face of the bluffbody. A fully developed pipe flow profile is imposed at the fuel stream boundary in order to closely capture the penetration of the fuel jet. At all the air stream boundaries, a plug flow profile is imposed. Further studies are needed to understand the sensitivity of the predictions on the profiles imposed on the fuel and air streams. The FDF transport model in conjunction with an augmented reduced mechanism for methane is used in the calculation of this flame. In order to balance computational effort and accuracy, five particles per cell are used in the simulation. However, to minimize stochastic errors, all particles in neighboring cells are also considered in the computation of ensemble means.

The augmented scheme (Table 1) is based on a 19-species 15-step C1 and C2 mechanism^[13]. Due to the complexity of this mechanism, integration of the kinetics equations is performed using ISAT. The objective of the ISAT scheme is to efficiently integrate the coupled set of reaction rate equations:

$$\frac{d\phi_{\alpha}(t)}{dt} = S_{\alpha}[\Phi(t)] \quad (3)$$

i.e., given the initial condition $\Phi(t_0)$, the reaction rate equation is integrated for a time $\Phi(t_0 + \Delta t)$. A table is built as the reactive flow calculation progresses, so that only the accessed region of the composition space is tabulated. Since the accessed region is a small subset of the realizable region, the dynamic creation of the table enables more efficient integration of the reaction equations than when the table is created *a priori* and the entire realizable region is tabulated. The accuracy of the ISAT integration is determined by a user specified tolerance parameter ϵ . In the present computations, a value of 10^{-4} was chosen for ϵ , to achieve acceptable accuracy levels. Calculations were performed on nine processors on a Linux machine and require approximately a month for full convergence of statistical quantities. The majority of the time was spent on chemistry computations and in achieving convergence of the statistical averages including those of trace species such as CO and NO.

Table 1. 19-Species, 15-Step Augmented Reduced Mechanism

$H+0.5O_2=OH$
$H_2+0.5O_2=H+OH$
$HO_2=0.5O_2+OH$
$0.5O_2+H_2O_2=OH+HO_2$
$0.5O_2+0.5C_2H_2=H+CO$
$CH_3+CO+C_2H_4=0.5O_2+CH_4+1.5C_2H_2$
$0.5O_2+2CH_3=H_2+CH_4+CO$
$0.5O_2+CH_3=H+CH_2O$
$0.5O_2+CH_4=OH+CH_3$
$0.5O_2+CO=CO_2$
$0.5O_2+C_2H_6=CH_4+CH_2O$
$H+OH=H_2O$
$H+CH_4+NO+HCN=0.5O_2+2CH_3+N_2$
$H+0.5O_2+CH_4+HCN=2CH_3+NO$
$0.5O_2+CH_4+NH_3+HCN=H_2O+2CH_3+N_2$

Figure 1 presents the instantaneous and time-averaged snapshot of the computed temperature field. The instantaneous temperature field shows an intermittent flame structure. The time-averaged field shows high temperatures in the near-field region and low temperature downstream. The near field of the bluffbody flame is characterized by two counter-rotating vortex rings (not shown in the figure) that help to stabilize the flame. Figure 2 shows the axial and radial velocities, respectively, at several axial stations in the flowfield. Note that the velocities are reasonably well predicted. Some discrepancies are seen in the radial velocities at far downstream locations that may be related to the coarseness of the grid near the exit boundary. Figure 3 shows the radial profiles of temperatures. In the near-field region, the temperatures are well represented; however, at $x = 120$ mm, peak temperatures are underpredicted. Similar features are also seen in the radial profiles of H_2 , CO , CO_2 and NO mass fractions (Figure 4). Overall, it can be seen that the predictions reproduce the data well. The near-field region is well-represented; however, some discrepancies are seen in the far-field region, which may be mitigated by increasing the grid resolution.

4. Gas Turbine Combustor

The application of LES to practical combustion systems is demonstrated by performing calculations of a gas turbine combustor. The computational domain consists of the region within the combustor liner only. The domain starts downstream of the swirler vanes. The swirl boundary conditions and liner primary and dilution port boundary conditions were determined by network analyses using measured pressure measurements on the combustor test-rig. The grid used in the calculations has

approximately 3 million hexahedral elements distributed across 20 processors on a Linux machine. The overall duration for each calculation was about three weeks.

The flow solver was linked to the assumed FDF combustion model described in Section 2 (B). Since liquid fuel is used in the combustor, a Lagrangian spray droplet transport and evaporation model^[2] was linked to the flow solver. Discrete size droplets were injected downstream of the fuel nozzle. These droplets were transported by the surrounding liquid and evaporated by the ambient air stream. The transport equations reflected the impact of droplet evaporation via source terms.

Two different liner wall port patterns (Mod A and Mod B) were analyzed (Figure 5). Mod A had two rows of holes on both inner and outer liner walls. Mod B had three rows of holes on the inner wall. Also, the size of the holes in the second row of the outer liner wall was reduced from Mod A. Figures 6 and 7 present the instantaneous contours of velocity magnitude and temperature in Mod A and Mod B, respectively. The dynamical features of the flow and reacting fields can be clearly seen. In comparison to Mod A, the higher airflow from the inner wall in Mod B results in lower temperatures close to the inner wall. Similarly, the lower airflow from the outer wall in Mod B results in higher temperatures close to the outer wall. Figure 8 presents circumferentially averaged fuel/air ratio versus span at the combustor exit from measurements and computations. It can be seen that the LES calculations reproduce the experimental trend reasonably well. In Mod A, RANS was also used to compute the exit profile. It can be seen from the figure that the prediction from LES is superior to that from RANS.

5. Summary

The paper presents applications of LES to laboratory flames and practical gas turbine combustors. LES of the bluffbody-stabilized turbulent hydrogen-methane flame was performed using the transport FDF model with a comprehensive augmented reduced mechanism that involved 19 species and 15 reaction-steps for the first time. The chemical mechanism involved both C1 and C2 species and was integrated using ISAT. Mean velocity and species/temperature fields were presented and compared to experimental data. Results showed that the computations are in good agreement with data. The paper also presents LES of a gas turbine combustor. Simulations of the combustor were performed using an assumed FDF turbulent-combustion model in conjunction with the flamelet-generated manifold method. Circumferentially averaged combustor exit fuel-air ratio profiles were compared to measurement data for two liner port patterns. It was shown that the LES calculations

were in reasonable agreement with data. These calculations indicated that LES of practical combustion systems is feasible and can be routinely used for design analyses.

Acknowledgments

This work was funded in part by a grant from the Indiana State 21st Century Research and Technology Fund. The Department of Defense High Performance Computing Modernization Program provided computational resources for the work presented in this paper.

References

- Leonard, A., "Energy cascade in large eddy simulations of turbulent fluid flows." *Advances in Geophysics A*, Vol. 18, p. 237, 1974.
- James, S., J.Zhu, and M.S. Anand, "Large eddy simulations as a design tool for gas turbine combustion systems." *AIAA J.*, 44, No.4, pp. 674-686, 2006.
- Moin, P. and S.V.Apte, "Large-eddy simulation of realistic gas turbine combustors." *AIAA J.*, 44, No.4, pp. 698-708, 2006.
- Menon, S. and N. Patel, "Subgrid modeling for simulation of spray combustion in large-scale combustors." *AIAA J.*, 44, No.4, pp. 709-723, 2006.
- Martin, C.E., L. Benoit, Y. Sommerer, F. Nicoud, and T. Poinsot, "Large-eddy simulation and acoustic analysis of a swirled staged turbulent combustor." *AIAA J.*, 44, No.4, pp. 741-750, 2006.
- Frankel, S.H., V. Adumitroaie, C.K. Madnia, and P. Givi, "Large eddy simulation of turbulent reacting flows by assumed PDF methods." In S.A Ragab, and . Piomelli, editors, *Engineering Applications of Large Eddy Simulations*, ASME, FED-Vol, 162, NY 1993.
- Givi, P., "Subgrid scale modeling in turbulent combustion: A review." *AIAA Journal*, 44, No. 1, (2006) 16-22.,
- James, S., Zhu, J., and M. S. Anand, "Large eddy simulations of turbulent flames using the filtered density function model." Accepted for the 30th *International Symposium on Combustion*, Heidelberg, Germany, 2006.
- James, S., Zhu, J., and M.S. Anand, "LES/FDF of turbulent flames using complex chemical kinetics." *AIAA-2006-4746*, 42nd AIAA/ASME/SAE/ASEE Joint Propulsion Conference, Sacramento, CA, 2006.
- Dally, B.B., A.R. Masri, R.S. Barlow, and G.J. Fiechtner, *Combust. Flame*, 114, pp. 119-148, 1998.
- Pope, S.B., "Computationally efficient implementation of combustion chemistry using in situ adaptive tabulation." *Combust. Theo. Modelling*, 1, pp. 41-63, 1997.
- Oijen, J.A. and L.P.H. van Goey, 17th *International Colloquium on the Dynamics of Explosions and Reactive Systems (ICDERS)*, Heidelberg, Germany, 1999.

- Sung, C.J., C.K. Law, and J. Y. Chen, "An augmented reduced mechanism for methane oxidation with comprehensive global parametric validation." In *Twenty-Seventh Symposium (Int'l) on Combustion*, The Combustion Institute, Pittsburgh, PA, pp. 295-304, 1998.

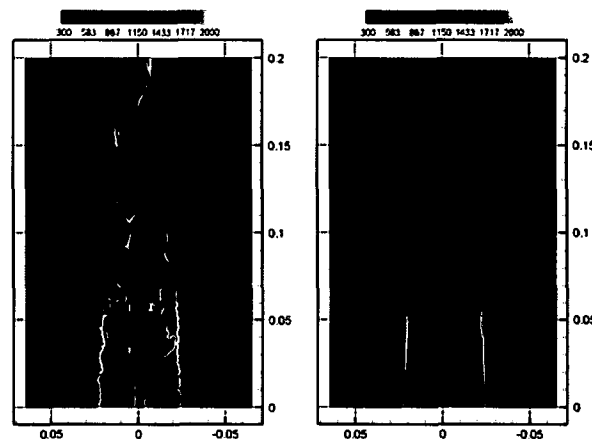


Figure 1. Computed instantaneous (left) and time-averaged (right) temperature fields in the HM1 burner

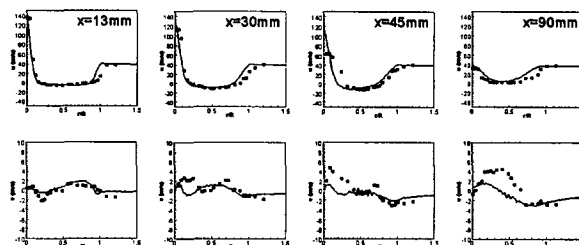


Figure 2. Comparison of axial (top) and radial (bottom) velocities with data in the HM1 burner

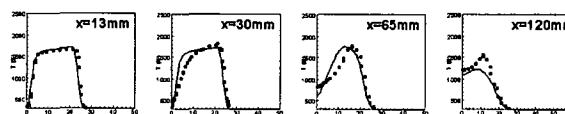


Figure 3. Comparison of predicted temperature against data for the HM1 burner

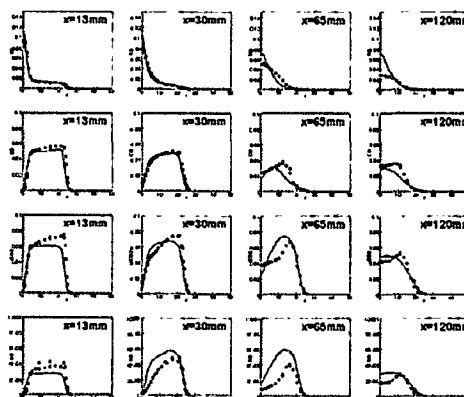


Figure 4. Comparison of predicted H₂, CO, CO₂ and NO mass fractions against data for the HM1 burner

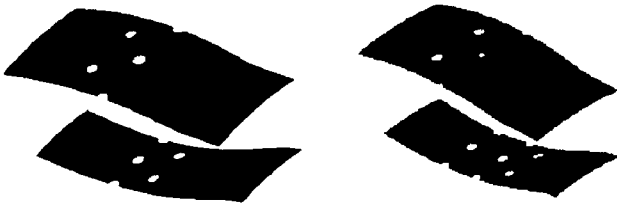


Figure 5. The two combustor liner hole configurations investigated; Mod A (left), Mod B (right)

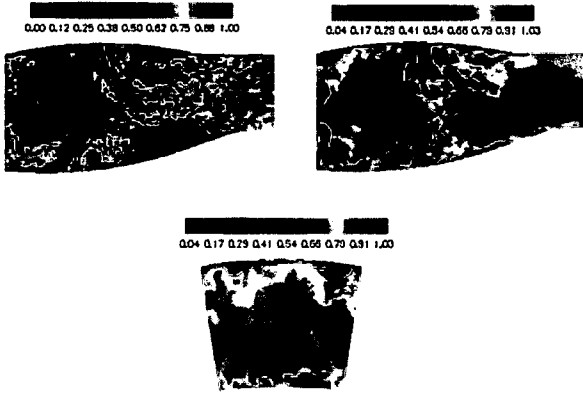


Figure 6. LES of Mod A combustor: instantaneous velocity magnitude (top left); instantaneous temperature (top right); instantaneous temperature at combustor exit (bottom). All units are normalized.

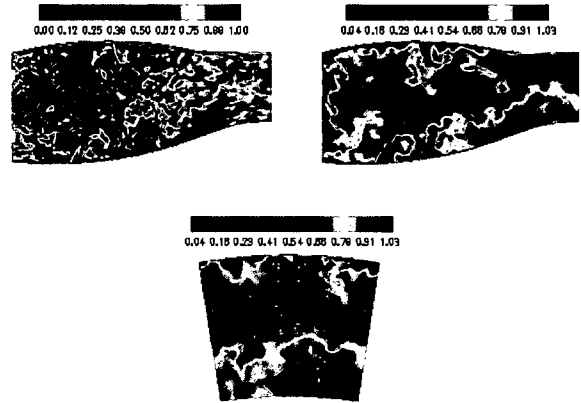


Figure 7. LES of Mod B combustor: instantaneous velocity magnitude (top left); instantaneous temperature (top right); instantaneous temperature at combustor exit (bottom). All units are normalized.

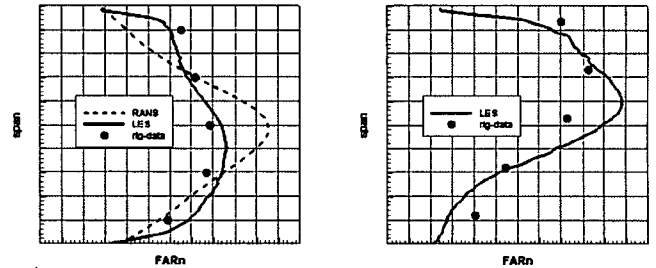


Figure 8. Circumferentially averaged normalized fuel-air ratio versus normalized span at the exit of the combustor: Mod A (left), Mod B (right)